Smart Structures and Systems, Vol. 3, No. 1 (2007) 115-131
DOI: http://dx.doi.org/10.12989/sss.2007.3.1.115

Double DOF control of an electromechanical integrated toroidal drive

Lizhong Xu† and Xin Liu

Mechanical Engineering Institute, Yanshan University, Qinhuangdao 066004, China

(Received March 12, 2005, Accepted October 20, 2006)

Abstract. The electromechanical integrated toroidal drive is a new drive system. For the control of the drive, the torque fluctuation and the steady-state errors should be removed and the fast response to the input change should be achieved. In this paper, the torque fluctuation of the drive system is analyzed and expressed as Fourier series forms. The transfer function of the torque control for the drive system is derived from its electromechanical coupled dynamic equations. A 2-DOF control method is used to control the drive system. Using definite parameter relationship of the 2-DOF control system, the steady errors of the torque control for the drive system is removed. Influences of the drive parameters on the control system are investigated. Using proper drive parameters, the response time of the control system is reduced and the quick torque response of the drive system is realized. Using a compensated input voltage, the torque fluctuation of the drive system is removed as well. The compensated input voltage can be obtained from the torque fluctuation equation and the transfer function. These research results are useful for designing control system of the new drive.

Keywords: toroidal drive; electromechanical integration; torque control; double freedom degree control.

1. Introduction

Toroidal drive can transmit large torque in a small size. They are suitable for applications in aviation and space flight fields. Some countries have been developing the drive for several years (Kuehnle 1996, Kuehnle, *et al*. 1981, Peeken, *et al*. 1984, Tooten 1985, Kuehnle 1999). As more electrical and control techniques are utilized in mechanical engineering fields, generalized composite drives will find new applications in advanced mechanical science. Electromagnetic harmonic drives (Delin and Huamin 1993) and piezoelectric harmonic ones (Barth 2000) are active drives in which the mesh between the flexible gear and the rigid gear are controlled by electromagnetic forces or piezoelectric forces. In the two drives, the drive and power are integrated.

Based on recent research (Xu and Huang 2003, Xu 2004), the authors develop a new electromechanical integrated toroidal drive which integrates control, power and toroidal drive (Xu and Huang 2005, Xu 2006).

The drive shown in Fig. 1 consists of four basic elements: (1) radially positioned planets; (2) the central worm; (3) a toroidal shaped stator; and (4) a rotor, which forms the central output shaft upon which the planets are mounted. The central worm is fixed. Coils are mounted in helical grooves of its

†Professor, Corresponding Author, E-mail address: Xlz@ysu.edu.cn

surface. The planets have permanent magnets instead of teeth. The N and S pole permanent magnets are mounted alternately on each planet. The stator has helical permanent magnets instead of helical teeth. In a same manner as the planet, the N and S pole helical permanent magnets are mounted alternately on the stator.

When a specific relationship is realized among the drive parameters, the N pole of one element will correspond to the S pole of the other elements. When the alternating voltage source is connected to the coils of the worm, a toroidal circular electromagnetic field is formed. It drives the several planets to rotate about their own axes. The magnetic forces between the teeth of the planet and stator cause the rotor to rotate about its own axis. Thus, the output power with a large torque at low speed is generated.

Compared with the toroidal drive, the new drive is easy to produce, is without wear, and does not need lubrication. It can be substituted for a servo system to simplify the structure of an existing electromechanical system. Besides the aforesaid fields that require compactness, the drive can be used with robots and in other fields that require accurate control.

Authors investigated the torques for the new drive (Xu and Huang 2005) and its control method under steady operating load (Xu 2006). As noted above, the drive can be used with robots and in other fields that require accurate control. The loads applied to the drive are complicated under certain conditions. Thus, for the control of the drive system, the rejection of disturbances and the fast response to the input change should be met simultaneously. For this, a two-degree-of-freedom(2-DOF) control system can be used. Many results about 2-DOF control of the electromechanical system can be found in the literature over the last twenty years. Liaw proposed a 2-DOF controller to improve control performance of the motor servo system (Liaw, *et al*. 1993, Lin, *et al*. 1995). Astrom and Hagglund proposed to design 2-DOF PID controllers with the maximum sensitivity of the closed loop (Astrom and Hagglund 1995). Taguchi and Araki tune 2-DOF PID control system in two steps based on the minimization of frequency response indices (Taguchi and Araki 1999). Raymond Gorez studied parameter design relations for 2-DOF control system (Gorez 2003). In references (Liaw and Lin 1995), 2-DOF control methods are combined with fuzzy control. In general, 2-DOF controls about the motor drive system have been investigated widely. However, when the 2-DOF control system is used in the electromechanical integrated toroidal drive, it should be noticed that there are three obvious differences between 2-DOF controls of the motor drive and the electromechanical integrated toroidal drive:

(1) The electromechanical integrated toroidal drive is an electromechanical integrated system. In operation of the drive system, the meshing tooth pair number between planet and stator or worm is variable. So, under the stable voltage, the output torque of the drive system will be variable as well. Therefore, the torque fluctuation in the drive system should be investigated and removed by control system.

(2) There are some essential differences between transfer functions of the motor drive and the electromechanical integrated toroidal drive. For the motor drive, the input voltage is connected to stator coils; for the new drive, the input voltage is connected to worm coils. For the motor, the output is the speed of the rotor which is identical to speed of rotating magnetic field; for the new drive, the output is also the speed of the rotor which is different from speed of rotating magnetic field. The output speed multiplied by speed ratio equals to the speed of rotating magnetic field. Hence, for the new drive, the output speed is low and the output torque is large. It is just the advantage of the new system over standard motor. Hence, the transfer function of the new drive system is affected by more factors such as pole pair number, turn number of the worm coils, tooth number of the planet and planet number, tooth number of the stator, planet radius, center distance between the planet and worm, etc. Influences of these

factors on the control performance of the drive system should be investigated as well. Therefore, another main task of the paper is transforming control function for the complicated system into a simple standard form.

(3) As stated above, in operation of the drive system, the torque fluctuation occurs. Removing the torque fluctuation, the rejection of disturbances and the fast response to the input change should be done simultaneously. Hence, a 2-DOF control method should be combined with a control method removing the torque fluctuation.

In this paper, for favoring control analysis, the torque fluctuation is analyzed and expressed as Fourier series forms. From the electromechanical coupled dynamic equations, the transfer function of the torque control for the drive system is derived in which more affecting factors are included. First, a single DOF control model of the drive system is presented. By the control model, the total close-loop responses of the drive system to the step, ramp and accelerating inputs are presented. Results show that the steady-state errors in the responses and the torque fluctuations occur. In order to remove the steady-state errors, a double DOF control model is used in the new drive system. By the double DOF control model, the steady-state errors in the responses are removed. Besides this, a compensated input voltage is added and combined with the 2-DOF control method. The responses of the drive system to the torque fluctuation are removed, the rejection of disturbances and the fast response to the input change are obtained simultaneously as well. Influences of the related parameters on the control performance of the drive system are investigated as well. These research results are useful for the application of the drive system.

2. Torque fluctuation

From reference (Xu and Huang 2005), the output torque T_n of the new drive is given as below

$$T_n = \frac{1}{2}k_v mqRF_g^2\frac{d\Lambda_g}{d\zeta}\left(\frac{2p+z_0}{z_1}\right)\sum_{i=1}^{z_v}\frac{1}{\sqrt{1+\frac{z_1^2}{4p^2}\left(\frac{a}{R}-\cos\phi_1\right)^2}} \tag{1}$$

where k_v is distributed winding coefficient, q is coil number per polar on worm, R is radius of the planet, a is center distance of the drive, ϕ_1 is rotating angle of the planet, F_g is magnetic potential, $F_g = Ni_s$, N is turn number of the coils, i_s is current intensity, Λ_g is air gap magnetic conductance, ζ is relative displacement between two sides of the air gap, z_v is teeth number on part planet enveloped by worm, z_1 is tooth number of the planet, z_0 is tooth number of the stator, p is pole pair number of the worm coils.

The meshing tooth pair number is variable in operation of the drive. The fluctuation of the meshing tooth pair number causes fluctuation of the output torque. Eq. (1) can be used to calculate output torques and their fluctuations as shown in Fig. 2. The values of the parameters used in calculations are presented as shown in Table 1.

Under condition of the asynchronous mounting, torque fluctuation along with rotating angle ϕ_1 of the planet is shown in Fig. 2(a). Under condition of the synchronous mounting, torque fluctuation in Fig. 2(b). From Fig. 2 it is known: the torque fluctuation under asynchronous mounting is smaller than that under synchronous mounting.

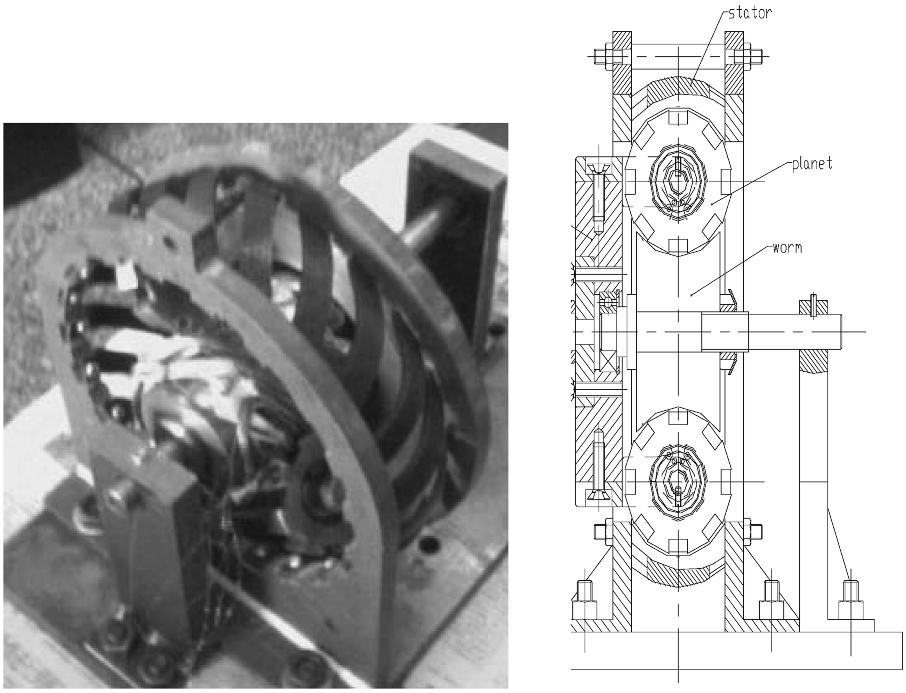

(a) Model machine of the drive (b) Mechanical drawing of the drive

Fig. 1 The electromechanical integrated toroidal drive

Table 1 Parameters for example drive

q (coil number per polar)	3
k_v (distributed winding coefficient)	3
R (planet radius)	30 mm
a/R (ratio)	2
B_0 (magnetic induction intensity)	1T
μ_0 (magnetic conductivity of free space)	$0.4\pi \times 10^{-6}$H/m
δ (airgap thickness)	1 mm
N (turn number of the coils)	100
i_s (current intensity)	9A
z_1 (tooth number of the planet)	8
z_0 (tooth number of the stator)	30
m (planet number)	4
p (pole pair number)	1

Above torque fluctuation can be calculated as below

$$T_n = \begin{cases} T_{\max} & 0 < \phi_1 < 5^{\circ} \\ T_{\min} & 5^{\circ} < \phi_1 < T^{\circ} - 5^{\circ} \\ T_{\max} & T^{\circ} - 5^{\circ} < \phi_1 < T^{\circ} \end{cases} \tag{2}$$

where $T_{\max}$ and $T_{\min}$ are the maximum output torque and the minimum output torque, respectively. T° is rotating angle period of the planet.

Under the load, the output torque is balanced by load torque T_j, thus

$$T_j = \frac{T_{\max} \cdot 10^{\circ} + T_{\min} \cdot (T^{\circ} - 10^{\circ})}{T^{\circ}} \tag{3}$$

From Eqs. (2) and (3), the torque fluctuation can be expressed as

$$\Delta \bar{T} = \begin{cases} \dfrac{T_{\max}}{T_j} - 1 = \Delta \bar{T}_1 & 0 < \phi_1 < 5^{\circ} \\ \dfrac{T_{\min}}{T_j} - 1 = \Delta \bar{T}_2 & 5^{\circ} < \phi_1 < T^{\circ} - 5^{\circ} \\ \dfrac{T_{\max}}{T_j} - 1 = \Delta \bar{T}_1 & T^{\circ} - 5^{\circ} < \phi_1 < T^{\circ} \end{cases} \tag{4}$$

In order to favor analysis, the torque fluctuation can be expressed as series form. From Fig. 2, it is known that the torque fluctuation function is even function. Hence, the torque fluctuation can be given as

$$\Delta \bar{T}(t) = a_0 + \sum_{n=1}^{\infty} a_n \cos n \omega_1 t \tag{5}$$

Here, the coefficient a_n can be calculated as below

$$a_0 = \frac{1}{T} \int_{-\frac{T}{2}}^{\frac{T}{2}} \Delta \bar{T}(t) dt = \frac{2}{T} \int_0^{\frac{T}{2}} \Delta \bar{T}(t) dt = \frac{2}{T} \left(\int_0^{T_1} \Delta \bar{T}_1(t) dt + \int_{T_1}^{\frac{T}{2}} \Delta \bar{T}_2(t) dt \right) = 0 \tag{6}$$

$$a_n = \frac{2}{T} \int_{-\frac{T}{2}}^{\frac{T}{2}} \Delta \bar{T}(t) \cos n \omega_1 t dt = \frac{\Delta \bar{T}_1 - \Delta \bar{T}_2}{n \pi} \sin n \omega_1 T_1 \tag{7}$$

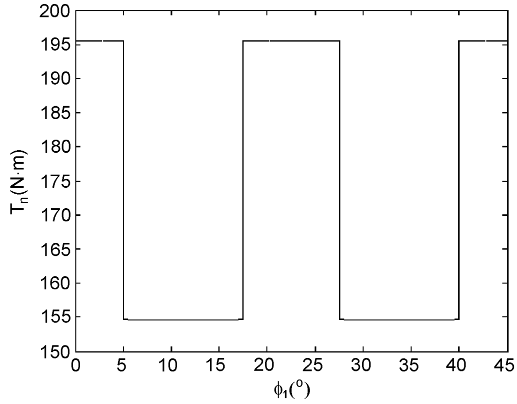

(a)

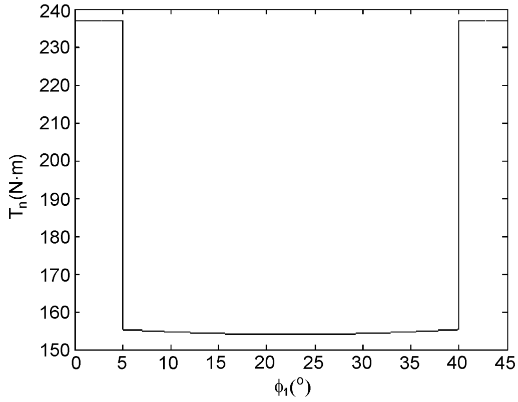

(b)

Fig. 2 The output torque fluctuation of the drive

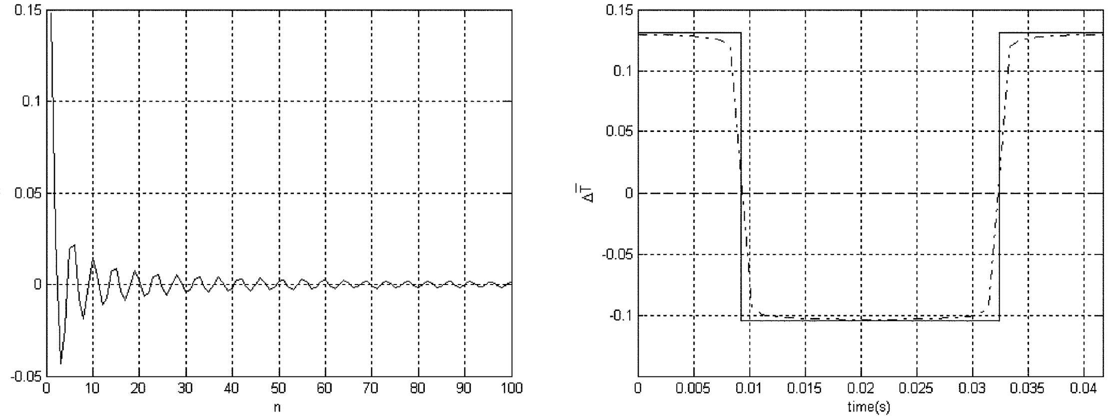

(a) Change of the coefficient for Fourier series along with its term number

(b) Comparison between the calculating and real torque fluctuations

Fig. 3 Comparisom between the calculating and real torque fluctuations

where T is time period of the speed fluctuation, $T = \frac{T^{o}}{\omega_0}$, ω_0 is steady speed of the rotor, T_1 is mutational point of the torque, $T_1 = \pi/36\omega_0$.

From Eq. (7), the change of the coefficient for Fourier series along with its term number is obtained as shown in Fig. 3(a). Fig. 3(a) shows that after the number of the terms of Fourier series is taken as $n = 45$, the coefficient will get to so small that they can be neglected. Hence, by Eqs. (5)-(7), the torque fluctuation are calculated and compared with real torque fluctuations as shown in Fig. 3(b)(here, $n = 45$). In Fig. 3(b), the broken curves show results calculated by Eqs. (5)-(7) and the solid lines shows the real torque fluctuations. From Fig. 3(b), it is known that the results given by Eqs. (5)-(7) are in good agreement with the real torque fluctuation.

3. Single DOF control model

The differential equations of the worm coils are as follows (Herbert, *et al.* 1968)

$$v_s = R_s i_s + (L_0 + L_2 \cos\theta)\frac{di_s}{dt} \tag{8}$$

where v_s, i_s and R_s are voltage, current intensity, and resistance of the ith phase worm coils, respectively. Here, L_0 is average value of self-inductance coefficient of the worm coils, L_2 is second harmonic amplitude of self-inductance coefficient of the worm coils.

From Eq. (1), the output torque T_n can be simplified as

$$T_n = k_t' i_s^2 \tag{9}$$

where $$k_t' = \frac{1}{2}k_v mqRN^2\frac{d\Lambda_g}{d\zeta}\left(\frac{2p+z_0}{z_1}\right)\sum_{i=1}^{z_v}\frac{1}{\sqrt{\left[1+\frac{z_1^2}{4p^2}\left(\frac{a}{R}-\cos\phi_1\right)^2\right]}}$$

Under the saturation of the magnetic circuit, the magnetic flux ϕ does not change with changing current, it can be given as

$$\phi = N i_0 \Lambda_g$$

where i_0 is saturation current.

Thus, the magnetic energy stored W_f can be calculated as below

$$W_f = i_s N \phi$$

Therefore, the magnetic force F across the air gap is

$$F = \frac{\partial W_f}{\partial \zeta} = N^2 i_0 i_s \frac{d\Lambda_g}{d\zeta}$$

From above equation, it is known that a linear relationship between force F and the current i_s is given. Substituting the force into the torque formula (Xu and Huang 2005), yields

$$T_n = k_t i_s \tag{10}$$

where
$$k_t = k_v mqRN^2 i_0 \frac{d\Lambda_g}{d\zeta}\left(\frac{2p+z_0}{z_1}\right)\sum_{i=1}^{z_v}\frac{1}{\sqrt{1+\frac{z_1^2}{4p^2}\left(\frac{a}{R}-\cos\phi_1\right)^2}}$$

As the drive operates normally under rated load, the magnetic circuit is under saturation condition. Hence, the torque control of the drive under the saturation of the magnetic circuit becomes the principal task for the control of the drive system. Therefore, in following analysis, a linear relationship between torque T_n and the current i_s is used.

From Eqs. (8) and (10), following equation can be obtained

$$k_t v_s = R_s \cdot T_n + (L_0 + L_2 \cos\theta) \cdot T_n' \tag{11}$$

From Eq. (11), the torque transfer function of the drive system is given as

$$G_T(s) = \frac{T_n(s)}{v_s(s)} = \frac{k_t}{L_v \cdot s + R_v} = \frac{K}{\tau \cdot s + 1} \tag{12}$$

where $L_v = L_0 + L_2 \cos\theta$ and $R_v = R_s$, τ is time constant, $\tau = \frac{L_v}{R_v}$, K is transfer function gain, $K = \frac{k_t}{R_v}$, the factors such as pole pair number, turn number of the worm coils, tooth number of the planet and planet number, tooth number of the stator, planet radius, center distance between the planet and worm, etc. are just included in the parameter K.

The feedback control model of the drive without controller is shown in Fig. 4. The responses of the drive system to unit step voltage, ramp voltage, accelerating voltage and torque fluctuation are presented, respectively, as shown in Fig. 5(here, $L_0 = L_2 = 10^{-2}H$, $R_s = 1.5\Omega$).

Figs. 5(a), (b) and (c) show the responses of the drive system to the step, ramp, and accelerating input

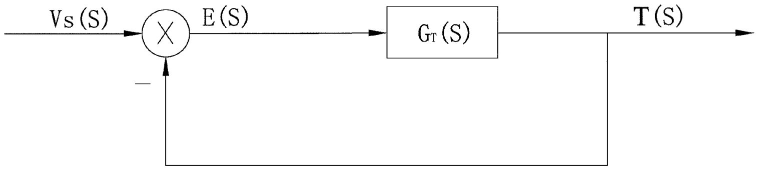

Fig. 4 Feedback control model of the drive without controller

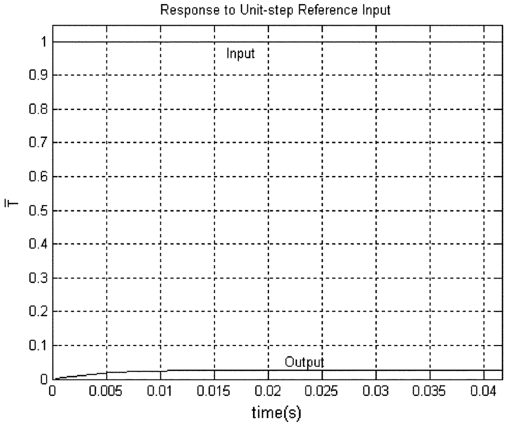

(a) Step input

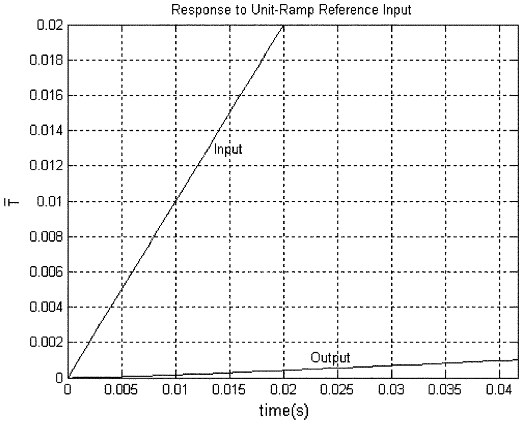

(b) Ramp input

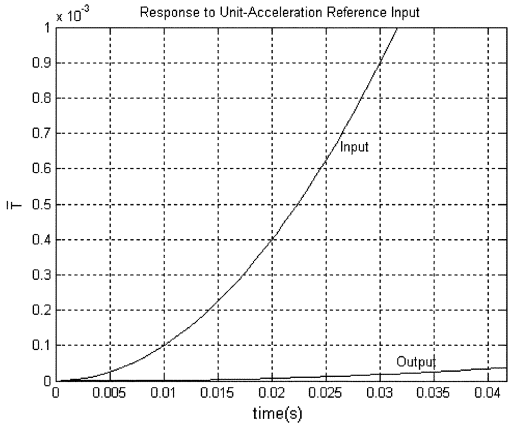

(c) Accelerating input

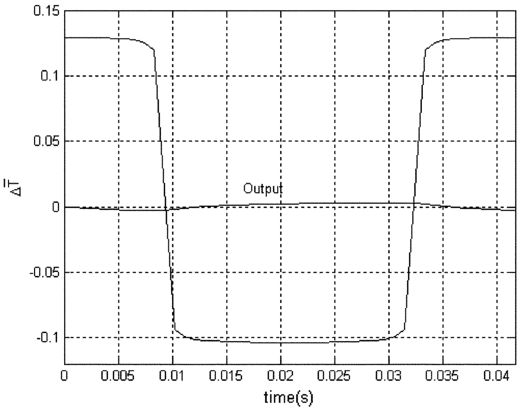

(d) Torque disturbance

Fig. 5 The responses of the drive system to voltage inputs and torque fluctuation

voltage under the condition that the torque fluctuation is not considered. Fig. 5(d) shows response of the drive system to the torque fluctuation. Figs. 5(a), (b) and (c) are superposed with Fig. 5(d), respectively, and then Figs. 6(a), (b) and (c) are obtained, respectively. Hence, Fig. 6 shows the total responses of the drive system to input voltage and torque fluctuation.

From Figs. 5 and 6, it is known that the steady-state errors in the responses of the drive system to the step, ramp, and accelerating input are quite large and the output torque fluctuation occurs as well. Besides this, it is also found that the drive system is an overdamping system and the torque responses are quite slow.

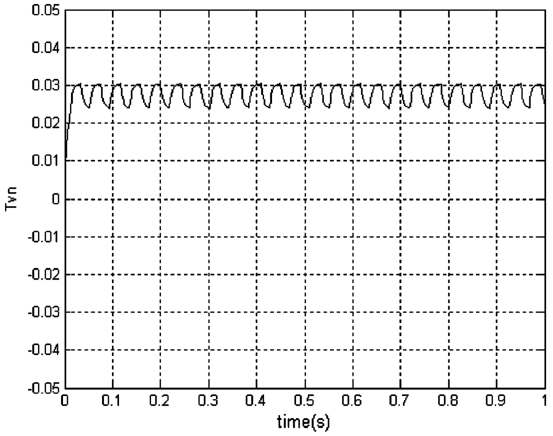

(a) Step input with torque disturbance

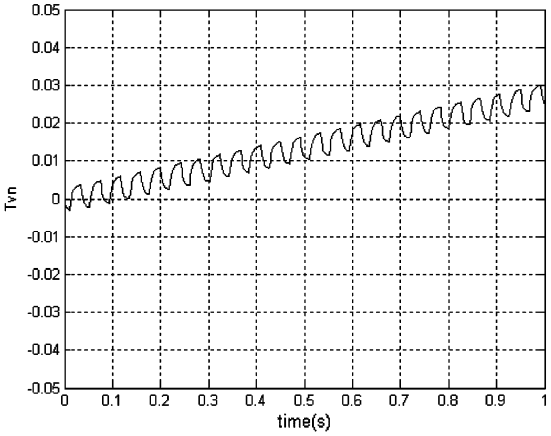

(b) Ramp input with torque disturbance

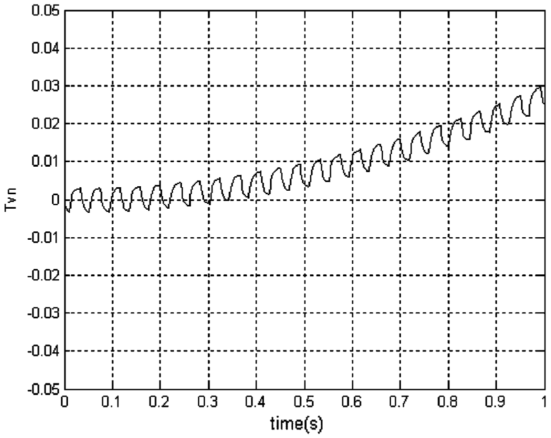

(c) Accelerating input with torque disturbance

Fig. 6 The total responses of the drive system to voltage excitations and torque fluctuation

In order that the drive system can be used with robots in which an accurate control is required, the fluctuation of the torque and the steady-state errors should be removed, and the quick control of the torque should be obtained. Therefore, for the new drive system, an effective control system should be investigated.

4. Double DOF control model

A double DOF control model is used to improve the torque control. Fig. 7 shows the structure of the control system, refined by the controllers.

In Fig. 7, T is the output torque of the rotor, v_s is the input control voltage, D is disturbing input, N is noise input, $G_T(s)$ is the transfer function of the drive system shown as Eq. (12), $G_{c1}(s)$ is the transfer function of the controller 1, which uses classical PID control algorithm

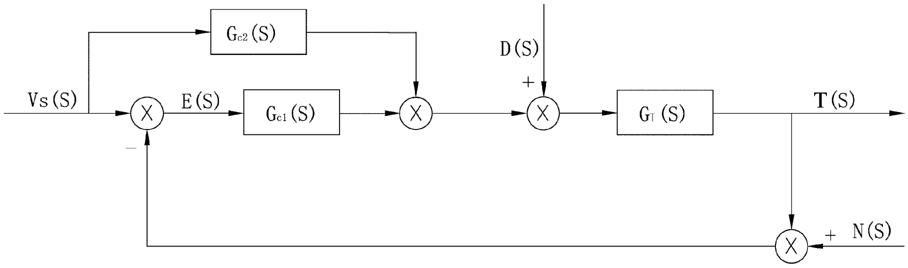

Fig. 7 Block diagram of the torque control system

$$G_{c1}(s) = K_p\left(1 + \frac{1}{T_i s} + T_d s\right) \tag{13}$$

$G_{c2}(s)$ is the transfer function of the controller 2, which uses classical P or PD control algorithm

$$G_{c2}(s) = K_p'(1 + T_d' s) \tag{14}$$

In Eq. (14), when $T_d' = 0$, $G_{c2}(s)$ becomes P controller.

Therefore, the closed loop torque transfer function $G_{Tv}(s)$, the disturbance transfer function $G_{Td}(s)$, and the noise transfer function $G_{Tn}(s)$ of the control system can be presented, respectively, as below

$$G_{Tv} = \frac{(G_{c1} + G_{c2}) \cdot G_T}{1 + G_{c1} \cdot G_T} \tag{15}$$

$$G_{Td} = \frac{G_T}{1 + G_{c1} \cdot G_T} \tag{16}$$

$$G_{Tn} = \frac{-G_{c1} \cdot G_T}{1 + G_{c1} \cdot G_T} \tag{17}$$

From Eqs. (15)-(17), the relationships among the three transfer functions can be given as

$$G_{Tn} = \frac{G_{Td} - G_T}{G_T} \tag{18}$$

$$G_{Td} = G_{Tn} \cdot G_{c2} + \frac{G_T - G_{Td}}{G_T} \tag{19}$$

From Eqs. (18)-(19), it is known that among the three transfer functions, two are independent. Hence, the control system is a double DOF control system. By the control system, more complicated control requirements can be met.

The transfer function $G_{c1}(s)$ of the controller 1 is taken as below

$$G_{c1}(s) = \frac{K_p(s+z)^2}{s} \tag{20}$$

Substituting Eqs. (14) and (20) into (15), yields

$$G_{Tv} = \frac{(G_{c1}+G_{c2})\cdot G_T}{1+G_{c1}\cdot G_T} = \frac{s^2K(K_p+K_p'\,T_d')+sK(2zK_p+K_p')+KK_pz^2}{s^2(\tau+KK_p)+s(1+2zKK_p)+KK_pz^2} \tag{21}$$

In order to remove steady-state errors in the responses of the drive system to the step, ramp, and accelerating input, let numerator of Eq. (21) equal last two terms of its denominator, yields

$$K_p+K_p'\,T_d' = 0 \tag{22}$$

$$K(2zK_p+K_p') = 1+2zKK_p \tag{23}$$

From Eqs. (22) and (23), parameters K_p' and T_p' of the transfer function $G_{c2}(s)$ are obtained

$$K_p' = \frac{1}{K} \tag{24}$$

$$T_d' = -KK_p \tag{25}$$

Substituting Eqs. (24) and (25) into (21), yields

$$G_{Tv} = \frac{2(2zKK_p)+KK_pz^2}{s^2(\tau+KK_p)+s(2zKK_p+1)+KK_pz^2} \tag{26}$$

Above related equations are used to analyze influences of the system parameters on the responses of the 2-DOF control system. The related results are shown in Fig. 8. From Fig. 8, it is known:

(1) Under condition that parameter relationship in Eqs. (24) and (25) are met, the tracking performance of the output torque to input signals is just realized. Under the condition, changes of the system parameters have not influence on the tracking performance of the output torque to input voltage.
(2) Under condition that parameter relationship in Eqs. (24) and (25) are met, changes of the system parameters have influence on response time and stability of the output torque to input signals.
(3) As the stator tooth number increases, the response speed of the control system increases and the its stability decreases.
(4) a/R is ratio of the center distance to planet radius. The ratio has obvious influence on response time and stability of the control system as well. As the ratio increases, the response speed of the control system increases and the its stability decreases.
(5) As the resistance of the circuit increases, the response speed of the control system decreases and the its stability increases.
(6) As the induction of the circuit increases, the response speed of the control system increases and the its stability decreases.
(7) As the parameters k_p and z increase, the response speed of the control system increases and the its stability decreases.
(8) In order to obtain quick response and good stability of the control system simutaneously, a team of moderate parameters should be used.

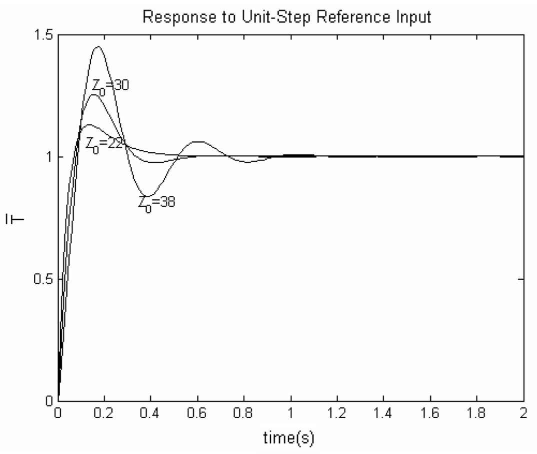

(a) influence of stator tooth number

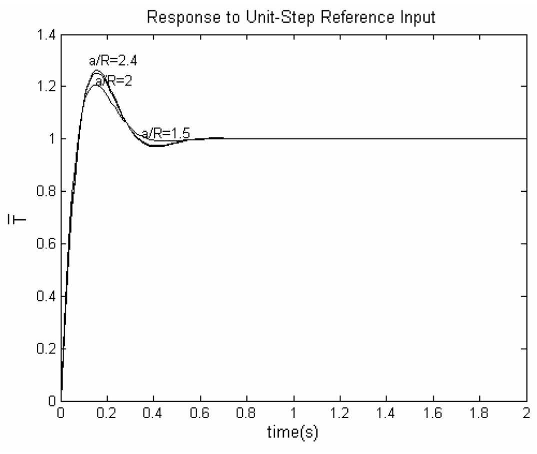

(b) influence of ratio a/R

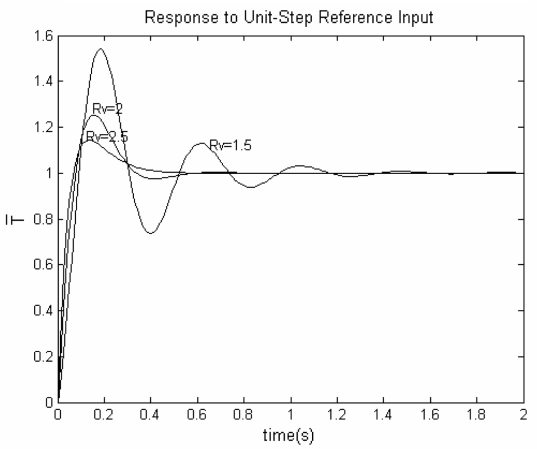

(c) influence of resistance

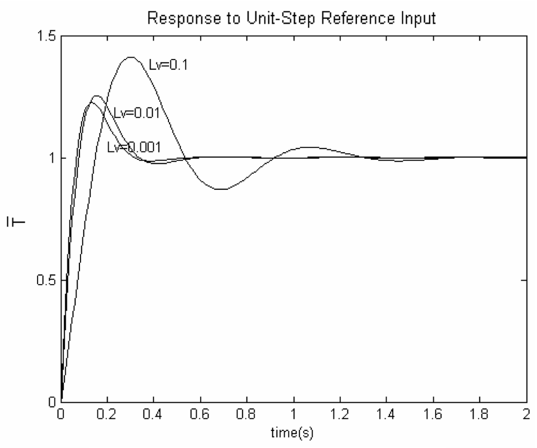

(d) influence of inductance

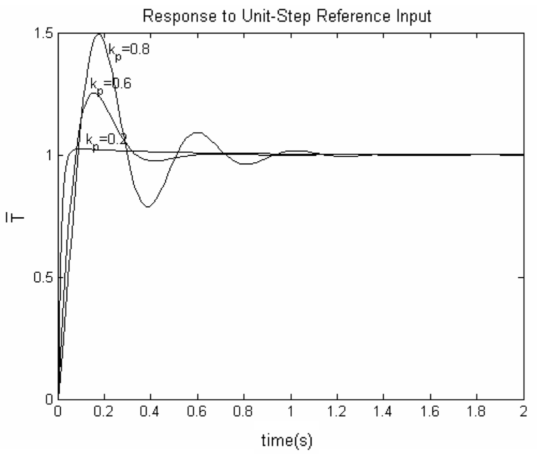

(e) influence of constant k_p

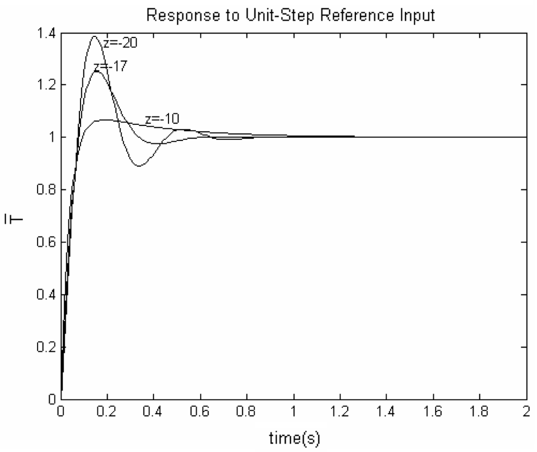

(f) influence of constant z

Fig. 8 Influences of the system parameters on the control performance

Table 2 Parameters of the controllers and system

K	τ	K_p	z
0.03	0.005	0.6	-17

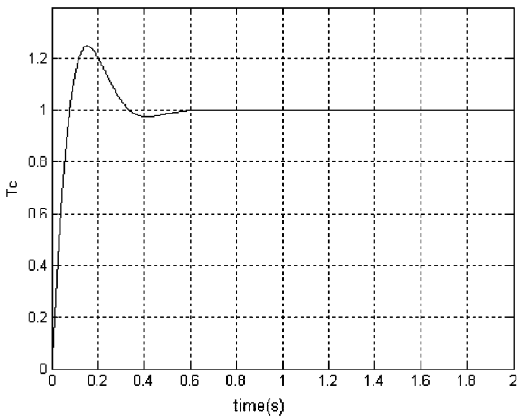

(a) Step input without torque disturbance

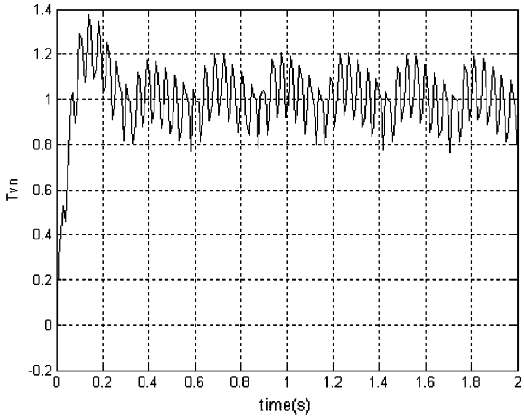

(b) Step input with torque disturbance

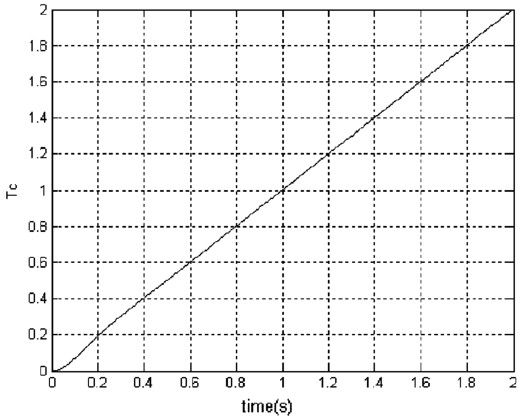

(c) Ramp input without torque disturbance

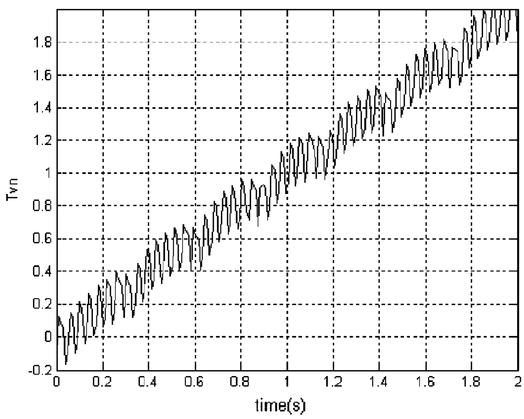

(d) Ramp input with torque disturbance

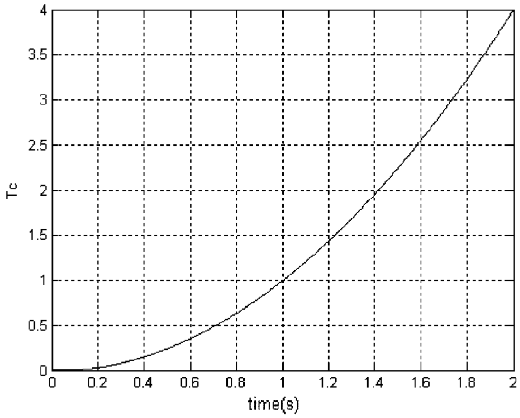

(f) Accelerating input without torque disturbance

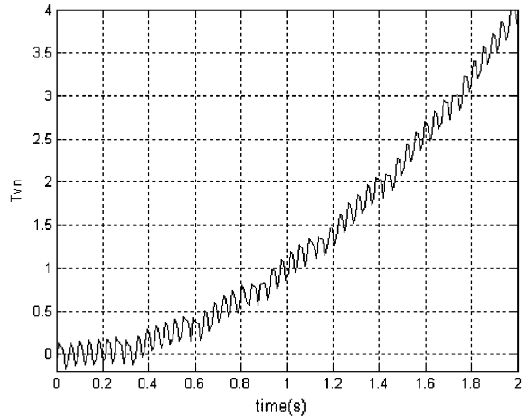

(e) Accelerating input with torque disturbance

Fig. 9 The closed-loop responses to step, ramp, and accelerating input

From analysis and calculation, a team of the parameters are selected in order to obtain quick response and good stability of the control system simutaneously under the condition that parameter relationship in Eqs. (24) and (25) are met. The parameters are shown in Tables 1 and 2.

Using the parameters, the responses of the 2-DOF control system to the step, ramp and accelerating inputs are analyzed. The simulations of these responses are shown in Figs. 9. Fig. 9(a, c) and (e) show responses without torque fluctuation, and Figs. 9(b, d) and (f) show responses with torque fluctuation. From Figs. 9(a, c) and (e), it is known:

(1) The steady-state errors in the responses of the control system to the step, ramp, and accelerating inputs are removed, and the good track performance of the control system with respect to step, ramp, and accelerating inputs is obtained.

(2) The control system is changed into underdamped system, and the response time is reduced and the quick response of the torque is obtained.

From Figs. 9(b, d) and (f), it is known:

(3) The output torque fluctuation caused by changes of the meshing tooth pair number has large influence on the responses of the control system. After the control system comes into steady state, the responses of the control system to torque fluctuation still occur.

(4) Based on the 2-DOF control system, the other measure should be used to remove the responses of the control system to torque fluctuation.

In order to remove the responses of the control system to torque disturbance, an adjusting input voltage $D(t)$ is applied to disturbing input end as shown in Fig. 10. Here, a differential link is added in the disturbing loop so that the adjusting input voltage $D(t)$ required becomes available control signals. From Fig. 10, it is known that the response of the control system to the compensation input voltage $D(s)$ should be equal to $-\Delta T(s)$. Therefore, the compensation input voltage $D(s)$ can be determined as below

$$D(s) = \frac{G_{c1}}{s}\Delta T(s) \tag{27}$$

Substituting Eqs. (5) and (20) into Eq. (27), the compensation input voltage $D(s)$ can be given.

$$D(s) = \sum_{n=1}^{\infty} K_p a_n \cdot \left(\frac{s}{s^2 + (n\omega_1)^2} + \frac{2z}{s^2 + (n\omega_1)^2} + \frac{z^2}{s(s^2 + (n\omega_1)^2)} \right) \tag{28}$$

From Eq. (28), the time-varying compensation input voltage $D(t)$ can be given as below

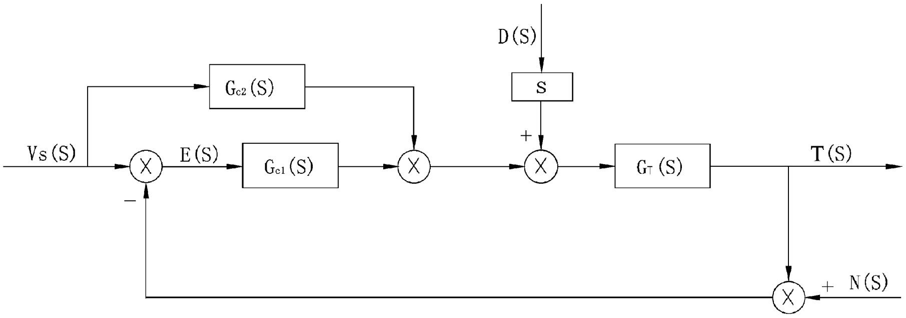

Fig. 10 Block diagram of the torque control system with voltage compensation

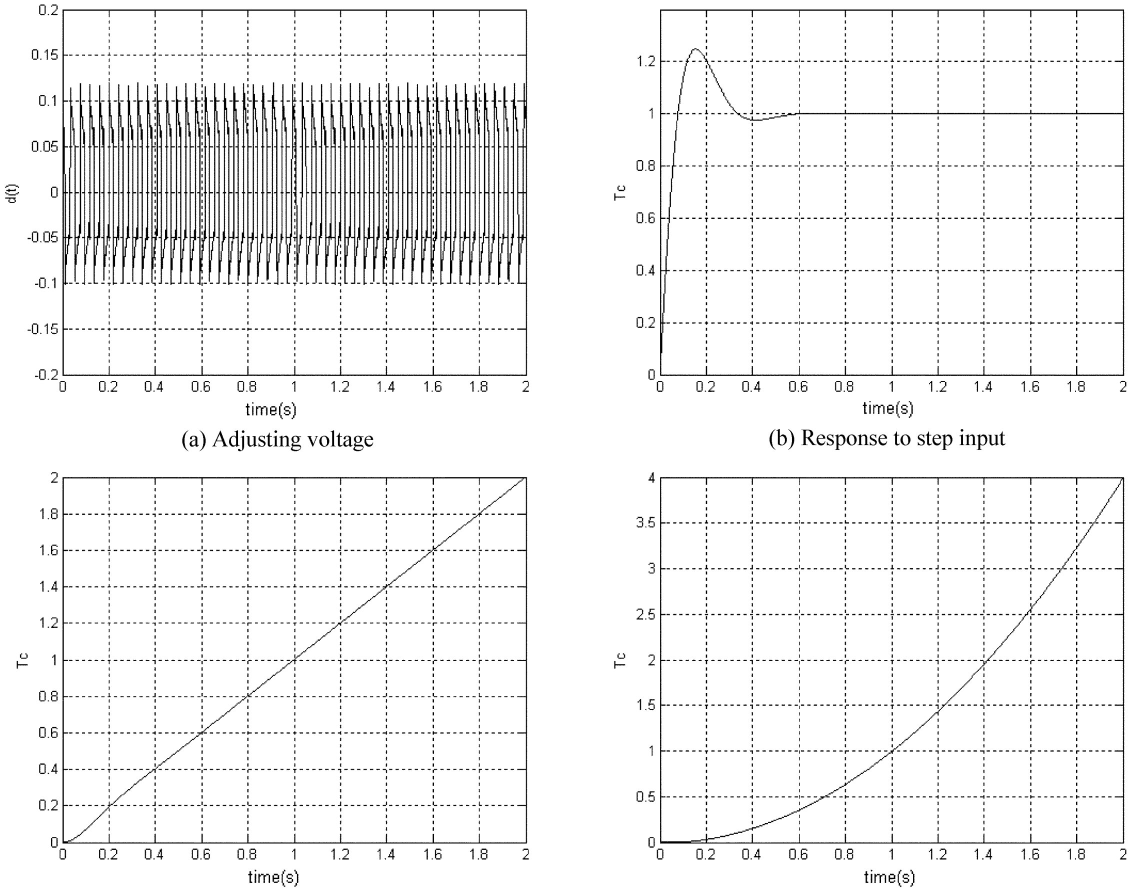

(a) Adjusting voltage (b) Response to step input

(c) Response to ramp input (d) Response to accelerating input

Fig. 11 Response of the feedback system with adjusting voltage

$$D(t) = L^{-1}[D(s)] = \sum_{n=1}^{\infty} Ka_n \cdot \left(\frac{z^2}{(n\omega_1)^2} + \left(1 - \frac{z^2}{(n\omega_1)^2}\right) \cdot \cos n\omega_1 t + \frac{2z}{n\omega_1} \cdot \sin n\omega_1 t \right) \tag{29}$$

By Eq. (29), the time-varying compensation input voltage $D(t)$ is obtained as shown in Fig. 11(a). Under compensation voltage, the responses of the 2-DOF control system to the step, ramp, and accelerating inputs are presented as shown in Figs. 11(b), (c) and (d). From Fig. 11, it is known:

(1) by compensation voltage, the responses of the 2-DOF control system to torque fluctuation are all removed and the steady output torque is all obtained under step, ramp, and accelerating inputs, respectively.

(2) Combining the compensation voltage with 2-DOF control system, not only above torque fluctuation are removed, but also the steady-state errors in the responses of the drive system to the step, ramp, and accelerating inputs are removed and the quick and stable torque control has been achieved as well.

(3) By aforementioned control method, the drive system will also have good tracking performance with respect to other input signals and steady errors will not occur. It makes the drive system suited to complicated operating condition of the robots.

5. Conclusions

In this paper, a 2-DOF controller is combined with a compensation input voltage and used to control the electromechanical integrated toroidal drive. By the control system, the torque fluctuation and the steady errors are removed, the quick and stable torque control is achieved. Here, the torque fluctuation in the drive system is presented from which the compensation input voltage can be derived. The definite parameter relationship of the two-DOF control system is given to remove the steady errors of the torque control. The parameters of the drive system have obvious influence on the total control system and they should be selected properly. These research results can be used to design the control system of the new drive subjected to the complicated loads.

Acknowledgements

This project is supported by the National Natural Science Foundation of China (No50375132).

References

Astrom, K. J. and Hagglund, T. (1995), "PID controllers: theory, design and tuning", Instrument society of America, Research Triangle Park, NC, U.S.A.

Barth, O. (2000), "Harmonic piezodrive-miniaturized servo motor", *Mechatronics*, **10**, 545-554.

Delin, Z. and Huamin, L. (1993), "Side surface harmonic stepper motor", *Chinese J. Mech. Eng.*, **29**(5), 96-98.

Gorez, R. (2003), "New design relations for 2-DOF PID-like control systems", *Automatica*, **39**, 901-908.

Kuehnle, M. R. (1966), Toroidgetriebe. Urkunde uber die Erteilung des deutschen Patents 1301682, Feb. 9.

Kuehnle, M. R. (1999), "Toroidal transmission and method and apparatus for making and assembling same", United States Patent 5863273.

Kuehnle, M. R., Peeken, H. and Troeder, C. (1981), "The toroidal drive", *Mech. Eng.*, **32**(2), 32-39.

Liaw, C. M. and Cheng, S. Y. (1995), "Fuzzy two-degree-of-freedom speed controller for motor driver", *IEEE Trans. Ind. Electron.*, **42**(2), 209-216.

Liaw, C. M. and Lin, F. J. (1995), "Position control with fuzzy adaptation for induction servomotor drive", *IEE Proc. –Electr. Power Appl.*, **142**(6), 397-404.

Liaw, C. M., Lin, F. J. and Kung, Y. S. (1993), "Design and implementation of a high performance induction motor servo drive", *IEE Proceedings-B*, **140**(4), 241-248.

Lin, F. J., Liaw, C. M., Shieh, Y. S., Guey, R. J. and Hwang, M. S. (1995), "Robust two-degree-of-freedom control for induction motor servo drive", *IEE Proc. Electr. Power Appl.*, **142**(2), 79-86.

Peeken, H., Troeder, C. and Tooten, K. H. (1984), "Berechnung und messung der lastverteilung im toroidgeriebe", *Konstruktion*, **136**(3), 81-86.

Taguchi, H. and Araki, M. (1999), "Effects of disturbance input point in two-degree-of-freedom PID control system", In preprints of the 42nd Japan Joint Automatic Control Conference. 239-242.

Tooten, K. H. (1985), Optimierung des Kraftubertragungsverhaltens in Getrieben mit Walzkon-takten", *Antriebstechnik*, **24**(7), 49-55.

Woodson, H. H. and Melcher, James R. (1968), *Electromechanical Dynamics*, John Wiley & Sons, INC. NEW YORK. LONDON SYDNEY.

Xu, L. (2004), “Efficiency for toroidal drive”, *Proceedings of the 11th World Congress in Mechanism and Machine Science*, April 1-4, Tianjin, China, 737-740.

Xu, L. (2006), “Design and torque control for electromechanical integrating toroidal drive”, *Mechanism and Machine Theory*, **41**(2), 230-245.

Xu, L. and Huang, J. (2006), “Torques for electromechanical integrating toroidal drive”, *Proceedings of the I MECH E Part C Journal of Mechanical Engineering Science*, **219**(8), 801-811

Xu, L. and Huang, Z. (2003), “Contact stresses for toroidal drive”, *J. Mech. Design. Transactions ASME*, **125**(3), 165-168.

JK